Bioconjugate Chemistry

Article

Cite This: Bioconjugate Chem. 2019, 30, 1150−1161

pubs.acs.org/bc

Dual Synthetic Peptide Conjugate Vaccine Simultaneously Triggers TLR2 and NOD2 and Activates Human Dendritic Cells

Gijs G. Zom,[†] Marian M. J. H. P. Willems,[‡] Nico J. Meeuwenoord,[‡] Niels R. M. Reintjens,[‡] Elena Tondini,[†] Selina Khan,[†] Herman S. Overkleeft,[‡] Gijsbert A. van der Marel,[‡] Jeroen D. C. Codee,[‡] Ferry Ossendorp,*[,†] and Dmitri V. Filippov*[,‡]

[†]Department of Immunohematology and Blood Transfusion, Leiden University Medical Center, P.O. Box 9600, 2300 RC Leiden, The Netherlands

[‡]Leiden Institute of Chemistry, Leiden University, Einsteinweg 55, 2333 CC Leiden, The Netherlands

Supporting Information

ABSTRACT: Simultaneous triggering of Toll-like receptors (TLRs) and NOD-like receptors (NLRs) has previously been shown to synergistically activate monocytes, dendritic cells, and macrophages. We applied these properties in a T-cell vaccine setting by conjugating the NOD2-ligand muramyl-dipeptide (MDP) and TLR2-ligand Pam_3CSK_4 to a synthetic peptide derived from a model antigen. Stimulation of human DCs with the MDP-peptide-Pam_3CSK_4 conjugate led to a strongly increased secretion of pro-inflammatory and Th1-type cytokines and chemokines. We further show that the conjugated ligands retain their ability to trigger their respective receptors, while even improving NOD2-triggering. Also, activation of murine DCs was enhanced by the dual triggering, ultimately leading to effective induction of vaccine-specific T cells expressing IFNγ, IL-2, and TNFα. Together, these data indicate that the dual MDP-SLP-Pam_3CSK_4 conjugate constitutes a chemically well-defined vaccine approach that holds promise for the use in the treatment of virus infections and cancer.

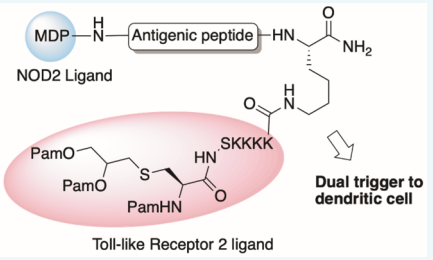

INTRODUCTION

During pathogenic infection, the innate immune system is exposed to a diverse array of pathogen-associated molecular patterns (PAMPs). Upon recognition of PAMPs by pathogen-recognition receptors (PRRs) such as the Toll-like receptors (TLR) and nucleotide-binding oligomerization domain (NOD)-like receptors (NLR), downstream signaling can generally lead to pro-inflammatory cytokine production by antigen-presenting cells (APCs) and increased expression of co-stimulatory proteins on their cell surface to optimize T cell activation.[1] The agonistic properties of TLR-ligands (TLR-L) have gained widespread interest in vaccine research as they can serve as immune-potentiating vaccine adjuvants.[2−4] Our group has shown that the potency of synthetic long peptide (SLP) vaccination can be strongly enhanced by conjugating the SLPs to TLR2-L Pam_3CSK_4 (Pam),[4] which effectuates the targeting of SLPs to TLR2-expressing APCs while concomitantly activating or maturing the APC.[5]

Muramyl-dipeptide (MDP), the minimal immune-stimulatory peptidoglycan component present in complete Freund's adjuvant,[6] is the cognate ligand of the cytosolic NLR, NOD2. Triggering of NOD2 ultimately results in activation of MAPK and NFκB.[7] Recently, we have studied the functionality of chemically well-defined NOD2-ligand MDP upon conjugation to synthetic long peptides (SLPs) and found that MDP retains its agonistic activity upon conjugation,[8] while the processing of SLPs by dendritic cells was not hampered by conjugation of MDP. Addition of a lipid side chain to MDP strongly enhanced its functionality as a DC- and macrophage-maturing agent, most likely explained by an enhanced uptake and subsequent higher abundance in the cytosol where the NOD2 receptor is located.[9−11]

Depending on the different input of signals and expression levels of receptors by an APC, the response of the APC will vary accordingly and may result in either a predominant Th1-, Th2-, or Th17-type response or an anti-inflammatory response.[12,13] Simultaneous triggering of different PRRs, such as combined TLR- and NLR-triggering, can induce synergistic effects. The first clues of this synergism derived from studies published in 1979 and 1987 in which guinea pigs experienced an enhanced endotoxic shock after inoculation with MDP and other bacterial cell-wall derived substances.[14] Increased lethality and anaphylactoid reactions were also observed in mice treated with LPS and MDP.[15] In the past decade, several groups have shown that a combination of NLR and TLR triggering synergistically enhances the secretion of pro-inflammatory cytokines by various cell types.[16−21] A few groups have specifically described the effects of combined triggering of NOD2 and TLR2, inducing synergistic cytokine release by various cell types.[22−30] The activation of dendritic

Received: February 1, 2019
Revised: March 12, 2019
Published: March 13, 2019

DOI: 10.1021/acs.bioconjchem.9b00087
Bioconjugate Chem. 2019, 30, 1150−1161

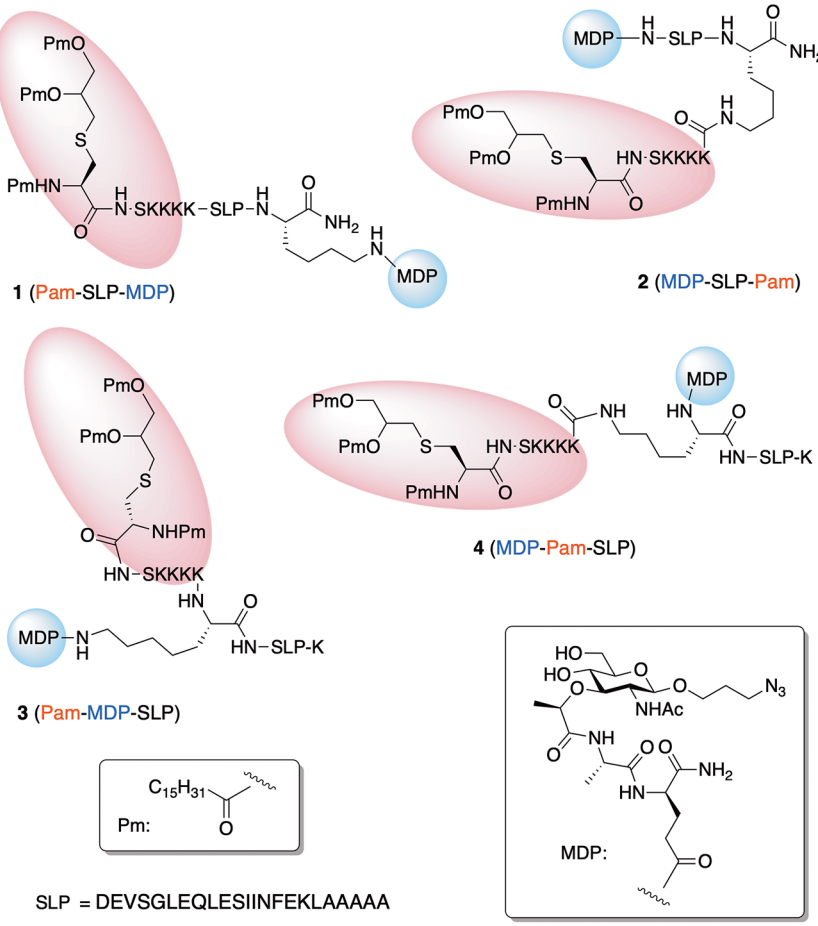

Figure 1. Dual conjugates (**1**−**4**) of four distinct structural types synthesized and investigated in this study. For the structures of the control constructs, see Supporting Information (SI) Figure S1.

cells (DCs), which play a pivotal role in the onset of adaptive immunity, can also be modulated by combined triggering of NOD2 and TLR, which synergistically enhances the secretion of inflammatory cytokines such as IL-12p70 and IFNγ.[31]

In the present study, we exploited the SLP platform to generate conjugates of both Pam_3CSK_4 and MDP conjugated to an SLP as a manner to modulate vaccine-induced innate and adaptive responses. Here we designed and synthesized four "dual conjugates" (conjugates **1**−**4**, Figure 1). In Pam-SLP-MDP conjugate **1**, the peptide (SLP) is elongated at the *N*-terminus with the TLR2-L, Pam_3CSK_4, while the side chain of the *C*-terminal lysine is connected with the isoglutamine of spacer containing MDP. Conversely, in MDP-SLP-Pam conjugate **2** the isoglutamine of MDP is attached to the *N*-terminus of the peptide epitope and Pam_3CSK_4 is bound to the side chain of the *C*-terminal lysine of the antigenic peptide. The Pam-MDP-SLP conjugate **3** and MDP-Pam-SLP conjugate **4** both contain a peptide that is provided with an additional lysine at the *N*-terminus to allow conjugation of both ligands on the same side of the conjugate via either the side chain or the α-amino function of the introduced lysine. For conjugate **3**, the α-amino function is elongated with the TLR2-L while the NOD2-L is connected to the side chain of lysine. In comparison with conjugate **3**, the linkages of the ligands with the epitope in conjugate **4** are reversed. We demonstrate that stimulation of human DCs by MDP-SLP-Pam **2** constructs leads to synergistic cytokine and chemokine release. In addition, we observe that murine T cells are induced to produce more IFNγ and IL-2 upon exposure to DCs pulsed with a MDP-SLP-Pam construct.

RESULTS

Synthesis of "Dual Conjugates" Containing Both NOD-L and TLR2-L Connected to Synthetic Long Peptide (SLP). The syntheses of conjugates **1**−**4** were largely carried out with an automated peptide synthesizer, using Fmoc-chemistry, the condensing agent HCTU and Tentagel-S-RAM as solid support. Commercially available protected amino acids and palmitoyl-Cys((*RS*)-2,3-di(palmitoyloxy)-propyl)-OH were used (Scheme 1). The syntheses of bis-conjugates **1**−**4** are depicted in Scheme 1 and require the availability of MurNAc derivative **8**, the preparation of which has been described previously.[8,9]

The syntheses of bis-conjugates Pam-SLP-MDP **1** and MDP-SLP-Pam **2** started with solid phase peptide synthesis (SPPS) of resin bound peptide **5**, having a *C*-terminal lysine equipped with the orthogonal and acid labile monomethoxytrityl (Mmt) protective group allowing *C*-terminal extensions at a later stage of the synthesis. To obtain conjugate **1**, TLR2-L Pam_3CSK_4 was attached to the *N*-terminus by elongation of peptide **5** with the SKKKK motive using a standard SPPS cycle, followed by a manual coupling with palmitoyl-Cys((*RS*)-2,3-di(palmitoyloxy)-propyl)-OH under influence of PyBOP and DiPEA resulting in immobilized peptide **6**. Subsequently,

DOI: 10.1021/acs.bioconjchem.9b00087
Bioconjugate Chem. 2019, 30, 1150−1161

Scheme 1. Synthesis of the Dual Conjugates 1−4[a]

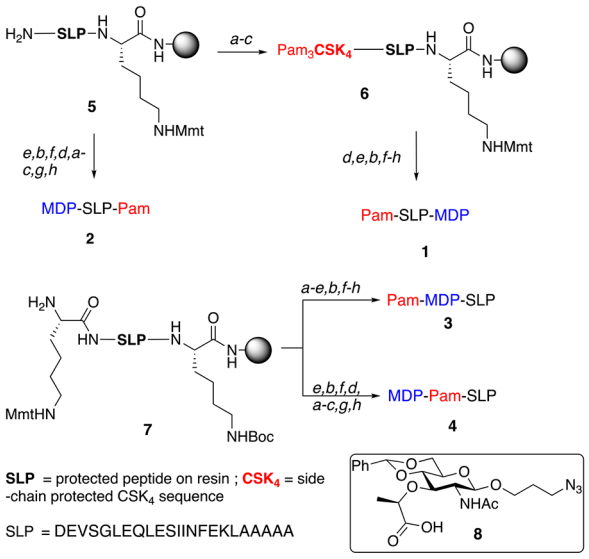

[a]Reaction conditions: (*a*) Fmoc SPPS cycle for SK_4; (*b*) 20% piperidine, NMP; (*c*) palmitoyl-Cys((*RS*)-2,3-di(palmitoyloxy)-propyl)-OH, PyBOP, DiPEA; (*d*) 3% TFA, DCM; (*e*) Fmoc SPPS cycle Fmoc-Ala-iGlu(NH_2)-OH; (*f*) **8**, HATU, DiPEA, NMP; (*g*) 95% TFA, 2.5% TIS, 2.5% H_2O; (*h*) RP-HPLC, yield conjugates: (**1**) 2.5 mg, 2%, (**2**) 0.94 mg, 1%, (**3**) 1.2 mg, 1%, (**4**) 1.5 mg, 1%.

immobilized peptide **6** was treated with a solution of 3% TFA in DCM to selectively remove the Mmt protective group at the side chain of the *C*-terminal lysine. To install the NOD2-L at this position, the free amine was consecutively elongated with Fmoc-isoglutamine, Fmoc-Ala-OH, and MurNAc derivative **8**. The coupling of **8** was executed twice using HATU instead of HCTU as condensing agent. Conjugate **1** was simultaneously deprotected and cleaved from the resin with a cocktail of 95% TFA, 2.5% TIS, and 2.5% H_2O for 60 min. The conjugate was precipitated with diethyl ether and purified by RP-HPLC yielding 2.5 mg Pam-SLP-MDP conjugate **1** in 2% overall yield.

To synthesize dual conjugate **2**, the NOD2-L was appended at the *N*-terminus of immobilized **5** by the above-described elongation with Fmoc-isoglutamine, Fmoc-Ala-OH, and MurNAc **8**. Next, the Mmt protective group at the side chain of the *C*-terminal lysine was selectively removed and the released amino group was extended with Pam_3CSK_4 by the same sequence of reactions as described for conjugate **1**. The thus obtained immobilized **2** was cleaved from the solid support, deprotected, and purified using the conditions as described for conjugate **1** to give 0.94 mg MDP-SLP-Pam conjugate **2** in 1% overall yield. The routes of synthesis to conjugates Pam-MDP-SLP **3** and MDP-Pam-SLP conjugate **4** have the immobilized peptide **7**, prepared by standard Fmoc SPPS, in common. The side chain of the *N*-terminal lysine in **7** is protected with the orthogonal Mmt protective group, permitting the successive addition of the TLR2 and NOD2 ligands. The sequence of reactions to install both the TLR2-L and NOD2-L in **3** and **4** was adopted from the synthesis of conjugate **1**. To obtain **3**, Pam_3CSK_4 was added to the free α-amine of **7**, followed by selective removal of the Mmt and appendage of NOD2-L at the side chain of lysine. To obtain conjugate **4**, NOD2-L was added to the free α-amine of **7**, followed by selective removal of the Mmt and attachment of Pam_3CSK_4 at the side chain of lysine. Acid treatment of the immobilized and protected precursors of **3** and **4** led, after precipitation and purification, to target Pam-MDP-SLP conjugate **3** and MDP-Pam-SLP conjugate **4**, both in 1% overall yield. The relatively low overall yields obtained for the syntheses of conjugates **1**−**4** can be explained by the concurrent hydrolysis of the azidopropyl group at the anomeric center of glucosamine of the NOD2-L.[8] The hydrolyzed side product hampered the final purification because of a small difference in retention time between the target conjugates **1**−**4** and their corresponding side products.

MDP-SLP-Pam Conjugate Induces Strongest NOD2-Triggering and Ensures Most Efficient Peptide Processing. Since we aimed to improve antigenic peptide-based T-cell vaccines by combining multiple PRR-triggers in one synthetic molecule, a number of assays were performed to assess the antigenicity of PRR-peptide conjugates that contain MDP, Pam_3CysSK_4 (Pam), and SLP in a 1:1:1 stoichiometry. Constructs consisting of either MDP or Pam conjugated to SLP (SI Figure 1) were used as control compounds. All conjugates (Figure 1) were based on an ovalbumin (OVA)-derived SLP, harboring the K^b-restricted CTL-epitope SIINFEKL. To identify the most optimal dual conjugate, murine DCs were incubated overnight with the indicated constructs (Figure 2A,B,C), after which the concentration of IL-12p40 in the supernatant was determined as a measure of DC activation (Figure 2A,B). The Pam-MDP-SLP, MDP-Pam-SLP, Pam-SLP-MDP, and MDP-SLP-Pam conjugates all showed strong induction of IL-12p40 induction by DCs (Figure 2A,B). MDP-SLP-Pam conjugate was most efficiently processed as shown by the activation of the SIINFEKL-specific T cell hybridoma (B3Z) after coculture with murine DCs loaded overnight with the indicated constructs (Figure 2C). The same conjugate also showed the strongest activation of human NOD2-transfected HEK293 cells after overnight stimulation (Figure 2D). Therefore, the MDP-SLP-Pam conjugate was selected as the most optimal construct and used in the subsequent experiments.

Synthetic Conjugates Composed of MDP, Pam_3CSK_4, and SLP Retain TLR2 and NOD2-Triggering Capacity. Confirming findings reported earlier in the literature, mixing of synthetic TLR2-L Pam_3CSK_4 and NOD2-L MDP induced synergistic activation of human monocyte-derived DC (moDC), as measured by the production of IL-12p40 (SI Figure S2A). Addition of MDP to various concentrations of Pam_3CSK_4 (Pam) led to a synergistic enhancement of IL-12p40 secretion by these DCs. This synergism was not observed in the expression of activation marker CD86 and HLA-DR on the cell surface of DCs (SI Figure S2B).

To analyze whether the conjugates SLP-Pam and MDP-SLP have retained their ability to trigger TLR2 and NOD2, respectively, HEK293 cells transfected with either human TLR2 (Figure 3A) or NOD2 (Figure 3B) were stimulated for 24 h with the conjugates described above, or with the single-ligand containing conjugates as controls. Both Pam and MDP can trigger their cognate receptor after conjugation to an SLP, as measured by secretion of IL-8 in the supernatant. However, TLR2-triggering was not enhanced by the dual conjugate MDP-SLP-Pam (Figure 3A). By contrast, the NOD2-expressing HEK293 cells show a clearly enhanced activation by the MDP-SLP-Pam construct as compared with their respective controls (Figure 3B). This is likely explained by enhanced cell entry and increased cytosolic presence of the

DOI: 10.1021/acs.bioconjchem.9b00087
Bioconjugate Chem. 2019, 30, 1150−1161

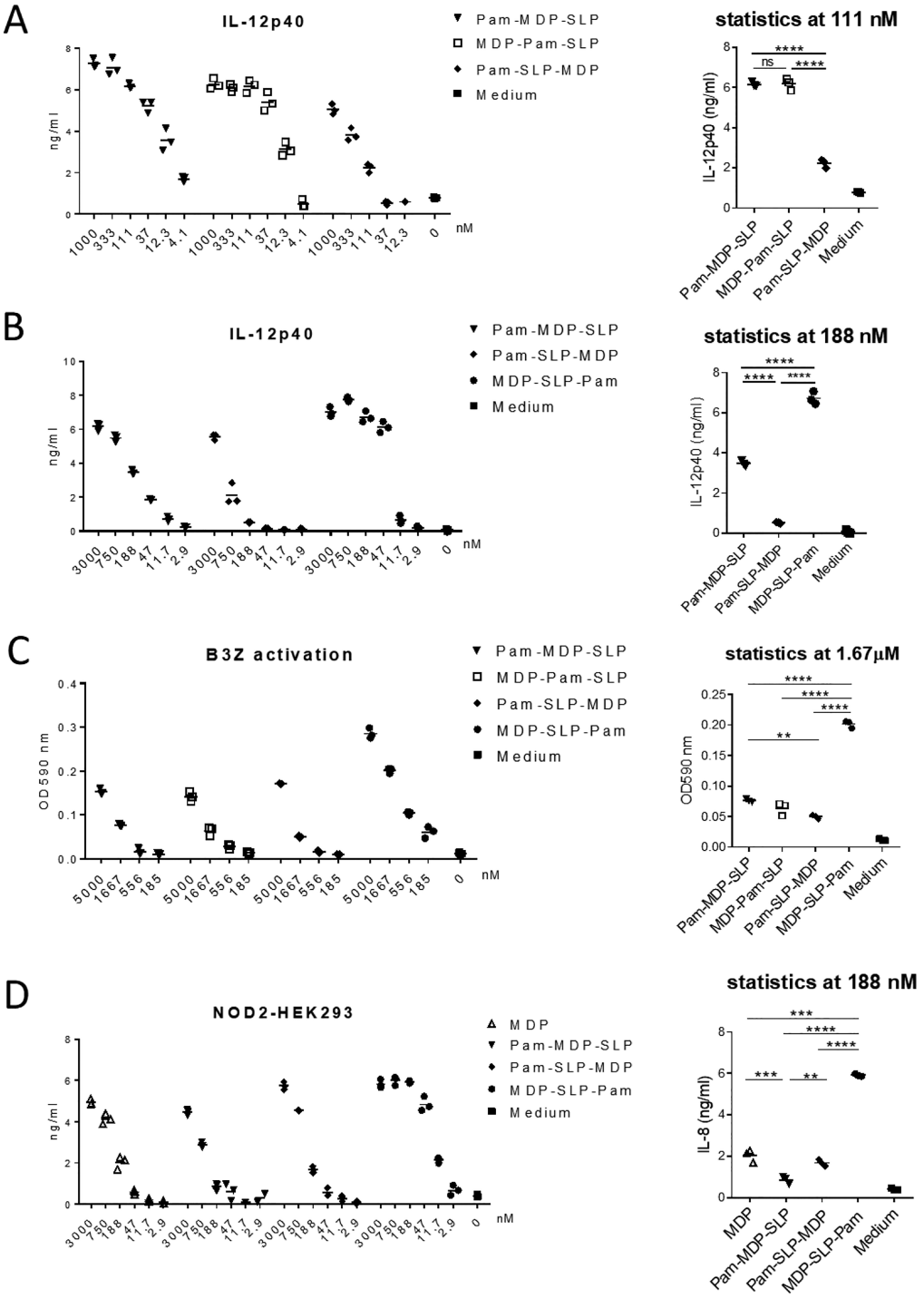

Figure 2. MDP-SLP-Pam conjugate optimally induces activation of DCs, NOD2-triggering, and peptide processing. (A,B) Concentration of IL-12p40 detected in the supernatant of murine DCs stimulated for 24 h with the indicated constructs. (C) Activation of T cell hybridoma B3Z recognizing the processed SIINFEKL CTL epitope embedded in the conjugated SLP_{OVA}, after overnight coculture with murine DCs previously loaded overnight with indicated constructs. Activation determined by colorimetric change after CPRG enzymatic conversion, OD measured at 590 nm. (D) hNOD2-HEK293 cell activation as determined by IL-8 production measured in the supernatant of cells incubated overnight with the indicated constructs. Depicted results are representative for 4 experiments conducted similarly with similar outcome. Significance determined by one-way ANOVA and Bonferroni post-hoc test. ** $p < 0.01$, *** $p < 0.001$, **** $p < 0.0001$.

MDP-SLP-Pam conjugate because of the lipidated nature of the constructs, as we have shown before.[9] As a control, wild-type nontransfected HEK293 cells were stimulated identically, which did not lead to IL-8 production (SI Figure S3). Together, these data show retained bioactivity of both TLR2- and NOD2-ligands upon N- or C-terminal conjugation to synthetic peptides.

Activation of Human DCs and PBMC by MDP-SLP-Pam Constructs Leads to Enhanced Cytokine Production. The combined triggering of receptors from different

DOI: 10.1021/acs.bioconjchem.9b00087
Bioconjugate Chem. 2019, 30, 1150−1161

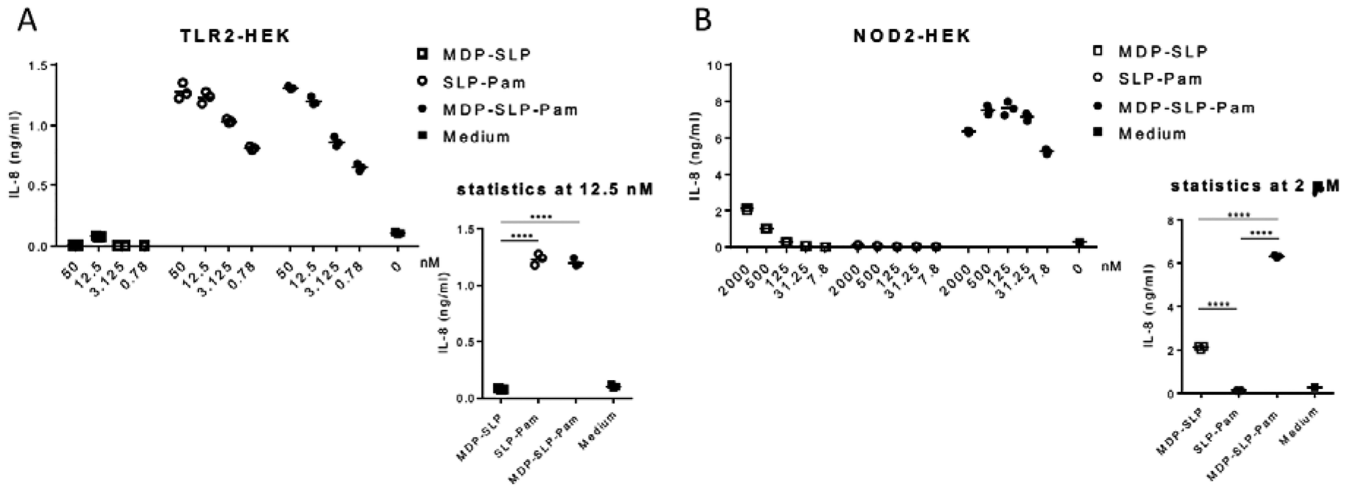

Figure 3. Pam_3CSK4 and MDP retain their ability to trigger their respective receptors upon conjugation to an SLP. (A) Detected concentration of IL-8 as a measure of receptor-mediated activation of HEK293 cells transfected with hTLR2 (A) or hNOD2 (B), after stimulation with the indicated titrated constructs containing an OVA-derived SLP. Significance determined by one-way ANOVA and Bonferroni posthoc test. **** $p < 0.0001$.

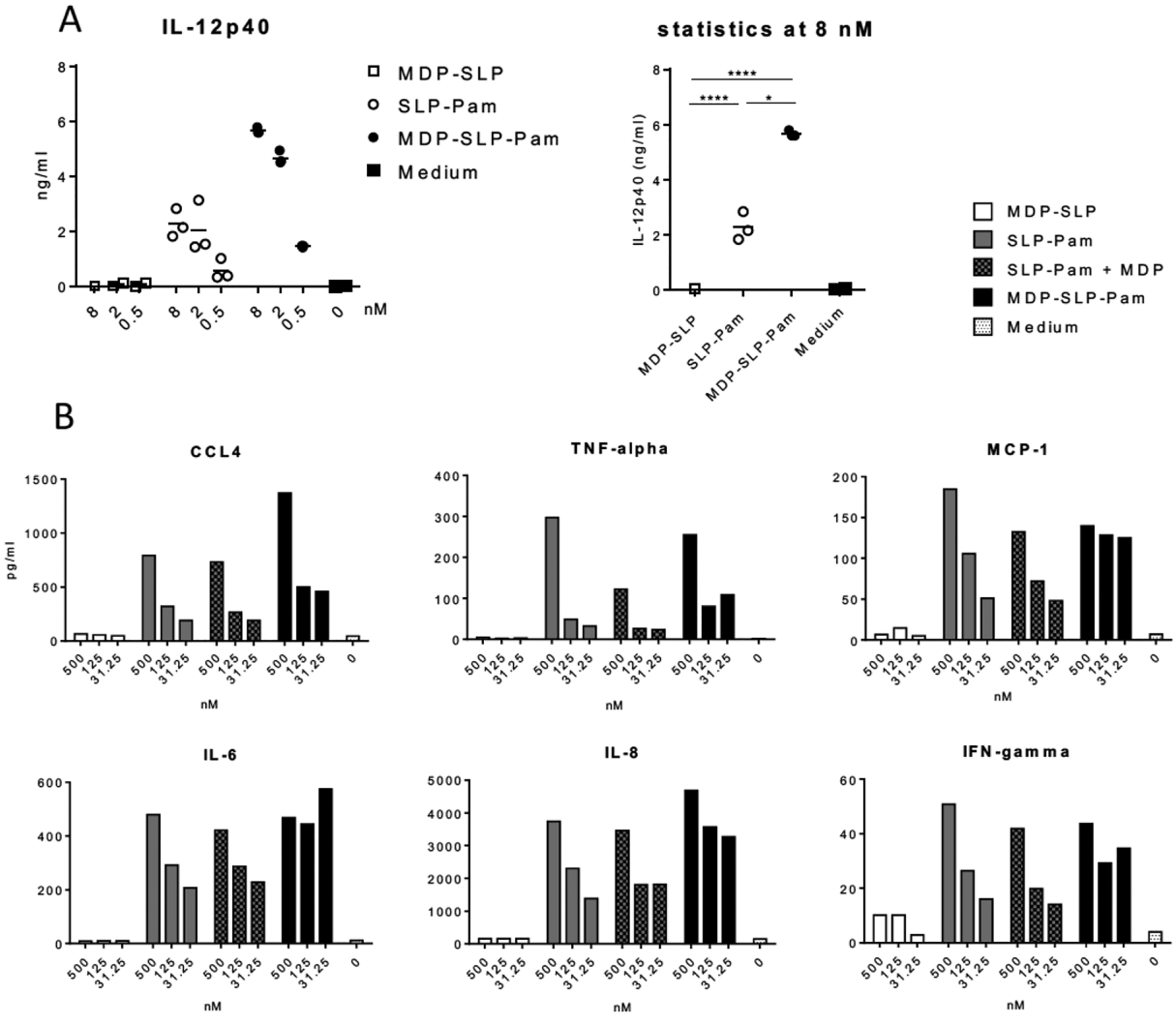

Figure 4. Cytokine and chemokine secretion profiles of human moDCs after stimulation with MDP-SLP-Pam constructs. (A) Concentration of IL-12p40 in supernatant of human moDCs incubated overnight with indicated constructs containing an OVA-derived SLP. (B) Cytokines and chemokines measured by Luminex in supernatants of moDCs stimulated with indicated MDP-SLP-Pam constructs. Representative results from 2 independently performed measurements. Significance determined by one-way ANOVA and Bonferroni posthoc test. * $p < 0.05$, **** $p < 0.0001$.

DOI: 10.1021/acs.bioconjchem.9b00087
Bioconjugate Chem. 2019, 30, 1150−1161

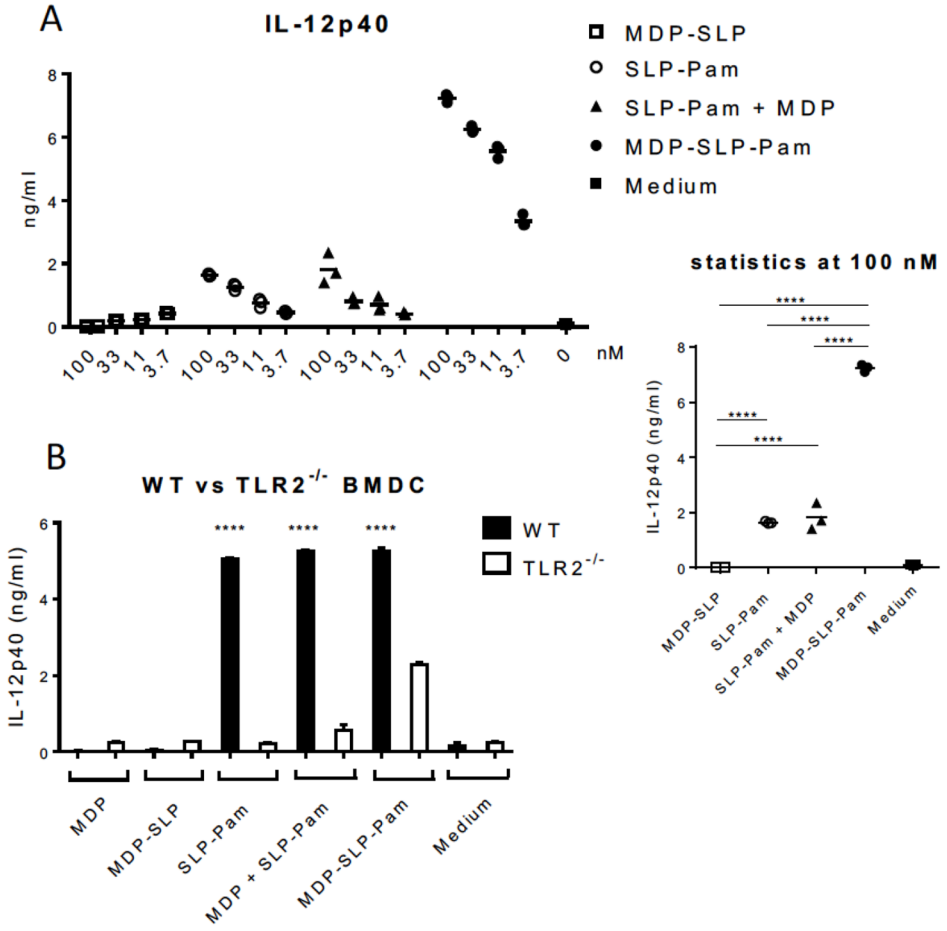

Figure 5. (A) Activation of murine DC cell line D1 as determined by measurement of secreted IL-12p40 in the supernatant after 16 h stimulation with MDP-SLP-Pam construct. (B) Activation of BMDCs derived and cultured from bone marrow from naïve WT or TLR2$^{-/-}$ C57BL/6 mice, after 16 h stimulation with MDP-SLP-Pam constructs and controls. All experiments were repeated at least twice resulting in a similar outcome. Significance in (A) determined by one-way ANOVA and Bonferroni posthoc test. Significance in (B) determined by unpaired *t* test for each construct. **** $p < 0.0001$.

PRR-families may skew the cytokine secretion profile of DCs. Therefore, the supernatant of human moDCs stimulated with the MDP-SLP-Pam construct and controls was analyzed using ELISA (Figure 4A) and Luminex (Figure 4B) to quantify the amounts of secreted IL-12p40, IL-6, IL-8, IFNγ, TNFα, MCP-1, and CCL4. Stimulation with the MDP-SLP conjugate did not induce secretion of any of the measured cytokines. In contrast, Pam conjugated to SLP (SLP-Pam) induced all measured cytokines. Although addition of free MDP to the SLP-Pam constructs did not enhance the effects induced by SLP-Pam alone, the dual MDP-SLP-Pam constructs strongly increased the expression of all cytokines. This is most likely explained by enhanced cellular uptake of the conjugated MDP upon conjugation to a lipid moiety, i.e., Pam. The levels of secreted IL-10 and IL-12p70 were also determined, which showed a similar trend as the other cytokines that were enhanced. However, the concentrations of the latter cytokines were all below 10 pg/mL and therefore not included in Figure 4. Overall, the dual conjugation of both Pam and MDP to an SLP induces a predominant inflammatory and Th1-associated immune response.

Murine DC Maturation Enhanced by Dual MDP-SLP-Pam Constructs. Murine assays provide a way to study the impact of the dual-conjugated SLPs on T cell priming. In Figure 5A, a murine DC cell line was stimulated with the MDP-SLP-Pam conjugate and controls for 24 h, after which the concentration of IL-12p40 was measured in the supernatant. Similar to what was observed for human DCs, murine DCs also produced significantly more IL-12p40 in response to stimulation with the MDP-SLP-Pam construct, while the mix of free MDP and SLP-Pam conjugate did not show synergy. Figure 5B shows maturation of murine bone marrow-derived DCs (BMDC), which are either of wild-type C57BL/6 origin or of a TLR2-deficient mutant on a C57BL/6 background. Maturation of BMDCs is clearly dependent on TLR2-expression, as maturation of the TLR2$^{-/-}$ BMDCs was lost or diminished after stimulation with any of the conjugates. Although the conjugation of MDP to these constructs did not enhance IL-12p40 production of the wild-type BMDCs, we did observe partial TLR2$^{-/-}$ BMDC activation after stimulation with the MDP-SLP-Pam conjugate (Figure 5B). This was also observed in the expression of CD40 and CD86 by TLR2$^{-/-}$ BMDC (SI Figure S4A). As a functionality control, the TLR2$^{-/-}$ BMDC could be adequately activated by stimulation with TLR9-L CpG to a similar extent as the WT BMDCs (SI Figure S4B).

DCs Loaded with MDP-SLP-Pam Construct Induce Enhanced CTL Priming. CD8$^+$ T cells derived from the transgenic mouse strain OT1 all recognize the SIINFEKL CTL epitope of OVA. After CD8$^+$ T cell enrichment of OT1

DOI: 10.1021/acs.bioconjchem.9b00087
Bioconjugate Chem. 2019, 30, 1150−1161

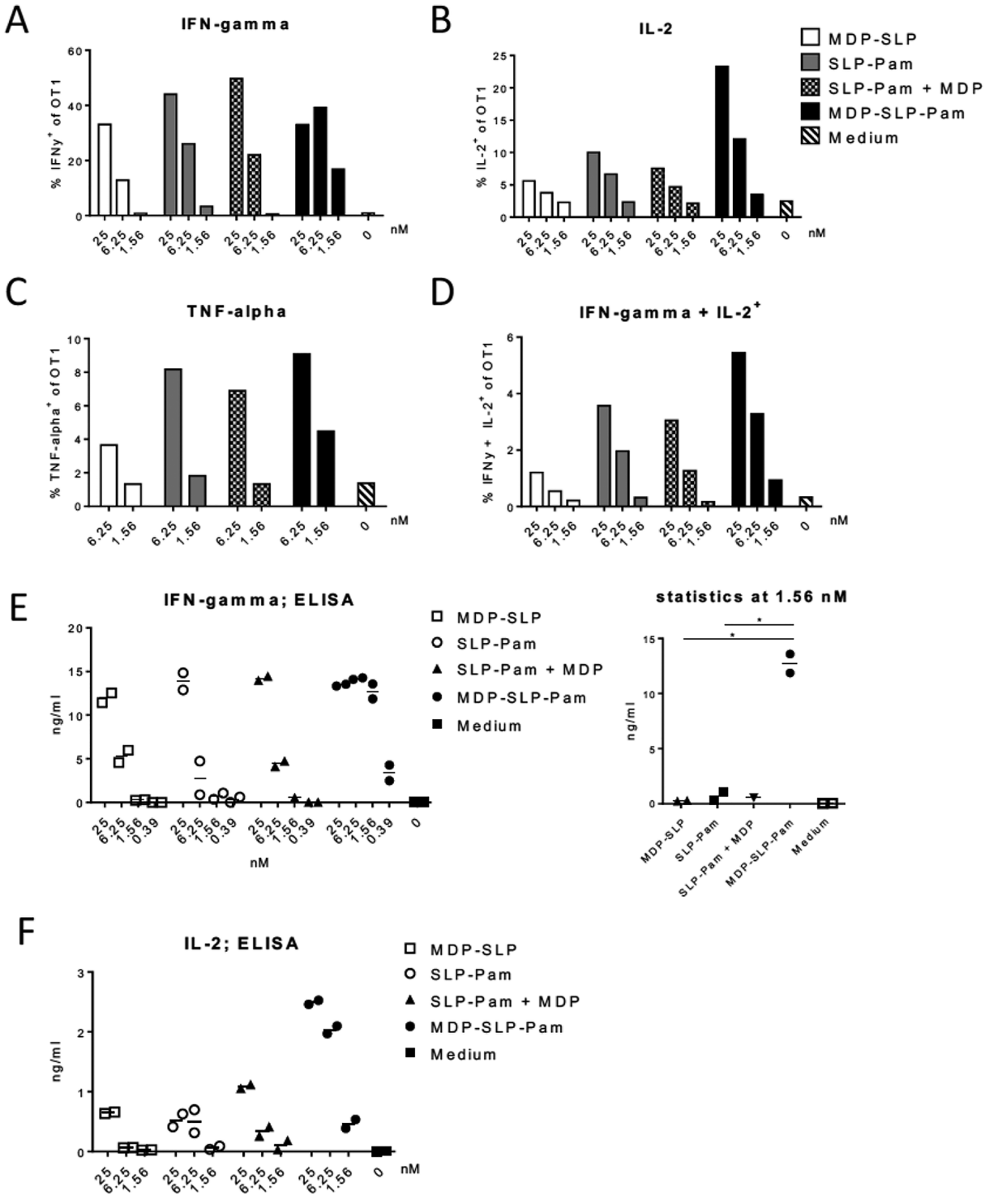

Figure 6. Enhanced specific T cell activation via murine DCs loaded with MDP-SLP-Pam construct. Activation of enriched transgenic OT1 $CD8^+$ T cells cocultured for 48 h with murine D1 DCs that had been stimulated overnight with indicated constructs containing an OVA-derived SLP. OT1 $CD8^+$ T cell activation determined by flow cytometric measurement of frequency of T cells with accumulated (A) IFNγ, (B) IL-2, (C) TNFα, and (D) both IFNγ and IL-2. Data from the same experiment indicating the concentration of (E) IFNγ and (F) IL-2 in the supernatant of cocultures as determined by ELISA. Experiment was repeated once resulting in a similar outcome. Significance in (E) determined by one-way ANOVA and Bonferroni posthoc test. * $p < 0.05$.

splenocytes and lymph node-derived cells, the OT1 $CD8^+$ T cells were added to washed murine DCs that had been incubated overnight with the MDP-SLP-Pam construct or controls. Subsequent intracellular cytokine staining revealed a strongly enhanced synthesis of IFNγ, IL-2, and TNFα by the OT1 exposed to DCs incubated with the MDP-SLP-Pam construct as compared with the control constructs (Figure 6A,B,C,D). In accordance with the increased number of $CD8^+$ T cells with intracellular cytokine production, the levels of secreted IFNγ and IL-2 detected in the supernatant were also

DOI: 10.1021/acs.bioconjchem.9b00087
Bioconjugate Chem. 2019, 30, 1150−1161

strongly enhanced after coculture of OT1 T cells with DCs loaded with the MDP-SLP-Pam construct (Figure 6E,F).

DISCUSSION

In the present study, we have characterized the properties of a dual synthetic peptide conjugate incorporating ligands for two different PRR families, e.g., NOD2-L MDP and TLR2-L Pam_3CSK_4. This first-of-a-kind synthetically designed conjugate vaccine induces an immune response with a pro-inflammatory and Th1-type biased immune signature which is of importance in the treatment of, e.g., cancer or (chronic) virus infections.

From an evolutionary point of view, cooperative signaling following from combined triggering of NOD2 and TLR2 makes sense as ligands for both receptors are derived from bacterial structures. The synergism arising after stimulation of both TLR2 and NOD2 has been studied extensively and mainly focuses on enhanced levels of cytokine secretion by various (mostly myeloid) cell types.[22−30] Different mechanisms for the synergy have been proposed: (1) MDP-induced upregulation of MyD88, lowering the threshold for subsequent TLR triggering,[22,24] and (2) converging signaling cascades downstream of both TLR and NOD2 triggering.[32] The latter mechanism involves the ubiquitination of NFκB essential modifier (NEMO) which is an essential step preceding NFκB activation. NEMO ubiquitination is partially mediated by TRAF6, an E3 ubiquitination ligase that is part of both TLR2 and NOD2 signaling cascades.[19,32] Also, the CARD-domain containing Rip2 kinase (Rip2K), which binds activated NOD2, contributes to activation of TRAF6-mediated MAP kinase pathways downstream of TLR2 triggering.[33]

Stimulation of human DCs by the MDP-SLP-Pam constructs led to synergistically enhanced levels of secreted cytokines (Figure 4) with a predominant pro-inflammatory signature (IL-6, IFNγ, TNFα) and chemokines (IL-8, MCP-1, and CCL4). CCL4 is known to recruit Th1-type naïve T cells, immature DCs, macrophages, and monocytes[34] while MCP-1 recruits memory T cells, monocytes, and macrophages, in addition to described pro- and antitumor effects.[35] The supernatant concentrations of IL-10 and IL-12p70 were below detection limits after stimulation with the MDP-SLP-Pam construct. The lack of IL-12p70 production was also described in a study by Tada et al., in which the authors observe synergism in IL-12p70 production by human DCs stimulated with MDP and several TLR-ligands (TLR3-L, TLR4-L, and TLR9-L) but not between MDP and TLR2-L.[31] Still, the MDP-SLP-Pam construct strongly tips the balance toward a pro-inflammatory and Th1-oriented cytokine profile when stimulating human DCs.

In mice, we observe efficient maturation of murine WT BMDCs by both the SLP-Pam and MDP-SLP-Pam constructs with no additive effect of the conjugated MDP. Murine BMDCs have a low activation threshold which may explain why the additive effect of MDP-conjugation is not observed. Although we did not determine the expression of NOD2 in these BMDCs, Yang et al. show that C57BL/6-derived $CD11c^+$ splenic DCs do express NOD2.[36] Also, the observation that MDP-SLP-Pam induces a partial maturation of the $TLR2^{-/-}$ BMDCs suggests that NOD2 is expressed in these cells (Figure 3C).

Strober and colleagues have previously shown that excessive Th1 responses can arise from mutations in the gene encoding for NOD2 (CARD15), which are frequently observed in Crohn's disease and inflammatory bowel disease (IBD) patients.[36−39] The authors claim that TLR2-induced activation of NFκB is inhibited by NOD2 activation, although others have come up with alternative or contradictory findings.[40−42] The molar concentrations of MDP used in the Strober studies are, however, roughly 10-fold higher than the molar concentrations of Pam_3CSK_4. By generating constructs in which one MDP-molecule and one Pam_3CSK_4-molecule are coupled to one SLP in our study, we probably prevent MDP-mediated overstimulation of APCs such as observed by Strober et al. Borm and colleagues specifically focused on dosage effects of MDP and found that TLR2-primed monocytes upregulated their cytokine secretion in response to low doses of MDP, whereas a high dose of MDP downregulated the responses.[43] Moreover, in our hands stimulation of moDCs using 80-fold higher concentrations of free MDP (20 μM) than free Pam_3CSK_4 (0.25 μM) also led to significantly enhanced levels of IL-12p40 production (data not shown).

Dendritic cells stimulated with the MDP-SLP-Pam construct improved specific $CD8^+$ T cell activation *in vitro* (Figure 6).

CONCLUSION

In conclusion we have described for the first time the synthesis and *in vitro* evaluation of conjugates consisting of ligands for both NOD2 and TLR2-L attached to an antigenic peptide with a class-I epitope sequence embedded. The data on the immunogenicity of the most active conjugate MDP-SLP-Pam indicate that such a construct not only improves activation of the antigen specific T-cells as compared to monoconjugates but also predominantly stimulates a proinflammatory and Th1-type response. This means that the MDP-SLP-Pam constructs have the potential to be applied as a vaccine against, e.g., (chronic) virus infections and tumors. In both cases, Th1-type responses characterized by specific CTL activation, adequate cytotoxicity and production of cytokines such as IFNγ, TNFα, and IL-2 are required for eradication of affected cells. This sets the stage to analyze whether MDP-SLP-Pam constructs also induce functional T cell responses *in vivo*.

EXPERIMENTAL PROCEDURES

Synthesis of MDP-SLP-Pam Constructs. All reagents and solvents used in the solid phase peptide synthesis were purchased from Bachem and Biosolve and used as received. Palmitoyl-Cys((*RS*)-2,3-di(palimitoyloxy)-propyl)-OH was purchased from Bachem, Fmoc-amino acids from Novabiochem. Free MDP-OH (**3S**), MDP-SLP (**1S**) conjugates (SI Figure 1) were prepared as described[8] as well as Pam_3CSK_4 (**4S**).[44] Tentagel based resins were ordered from Rapp Polymere. Light petroleum ether with a boiling range of 40−60 °C was used. All other solvents used under anhydrous conditions were stored over 4 Å molecular sieves except for methanol, which was stored over 3 Å molecular sieves. Solvents used for work-up and silica gel column chromatography were of technical grade and distilled before use. All other solvents were used without further purification. Reactions were monitored by TLC analysis or LC/MS analysis. LC/MS was conducted on a JASCO system using an Alltima C_{18} analytical column (4.6 × 50 mm, 5 μm particle size, flow 1.0 mL/min), Alltima CN analytical column (4.6 × 50 mm, 3 μm particle size, flow 1.0 mL/min), or a Alltima C_4 analytical column (4.6 × 50 mm, 5 μm particle size, flow 1.0 mL/min). Absorbance was measured at 214 and 256 nm. Solvent system: A: 100%

DOI: 10.1021/acs.bioconjchem.9b00087
Bioconjugate Chem. 2019, 30, 1150−1161

water, B: 100% MeCN, C: 1% aq. TFA. Gradients of MeCN in 10% C were applied over 15 min unless stated otherwise. Purifications were conducted on the Gilson GX-281 preparative RP-HPLC system, supplied with a semi preparative Alltima CN column (10 × 250 mm, 5 μm particle size, flow 5.0 mL/min) or semi preparative Alltima C_4 column (10 × 250, 5 μm particle size, flow 5.0 mL/min). Solvent system: A: 0.1% aq. TFA and B: MeCN. Gradients of 10−90% MeCN were applied over 3 CV over 15 min unless stated otherwise. The UV absorption was measured at 214 and 256 nm. High resolution mass spectra were recorded by direct injection (2 μL of a 2 μM solution in H_2O/MeCN; 50/50: v/v and 0.1% formic acid) on a mass spectrometer Thermo Finnigan LTQ Orbitrap equipped with an electrospray ion source in positive mode (source voltage 3.5 kV, sheath gas flow 10, capillary temperature 523 K) with resolution R = 60000 at m/z 400 (mass range m/z = 150−2000) and dioctyl phthalate (m/z = 391.28428) as lock mass. Optical rotations were measured on a Propol automatic polarimeter (sodium D-line, λ = 589 nm). Specific rotations $[\alpha]^D$ are given in degrees per centimeter and the concentration c is given in mg/mL in the specific solvent. Maturation and B3Z presentation results were analyzed with Graphpad Prism version 5.01 for Windows, GraphPad Software, San Diego, California, USA. IR spectra were recorded on a PerkinElmer Paragon 1000 FT−IR Spectrometer.

General Procedure for Automated Solid-Phase Synthesis. The solid-phase peptide synthesis was performed on a 50 μmol or 25 μmol scale according to established methods[8,45] on an ABI 433A (Applied Biosystems) automated instrument applying Fmoc based protocol starting from Tentagel-S-RAM resin (loading 0.23 mmol/g) or loaded with described peptide. The synthesis was continued with Fmoc-amino acids specific for each peptide. The consecutive steps performed in each cycle for HCTU chemistry on 50 μmol scale:

1. Deprotection of the Fmoc-group with 20% piperidine in NMP for 15 min. 2. NMP wash. 3. Coupling of the appropriate amino acid using a 5-fold excess. Generally, the Fmoc amino acid (0.25 mmol) was dissolved in 0.25 M HCTU in NMP (1 mL); the resulting solution was transferred to the reaction vessel followed by 0.5 mL of 1.0 M DiPEA in NMP to initiate the coupling. The reaction vessel was then shaken for 30 min. 4. NMP wash. 5. Capping with 0.5 M acetic anhydride in NMP in the presence of 0.5 mmol DiPEA. 6. NMP wash. 7. DCM wash.

Aliquots of resin of the obtained sequences were checked on an analytical Alltima C_{18} column (4.6 × 50 mm, 5 μm particle size, flow 1.0 mL/min). The Fmoc amino acids applied in the synthesis were as follows: Fmoc-Ala-OH, Fmoc-Asn(Trt)-OH, Fmoc-Asp(OtBu)-OH, Fmoc-Gln(Trt)-OH, Fmoc-Glu-(OtBu)-OH, Fmoc-Gly-OH, Fmoc-Ile-OH, Fmoc-Leu-OH, Fmoc-Lys(Boc)-OH, Fmoc-Lys(Mmt)-OH, Fmoc-Phe-OH, Fmoc-Ser(^{t}Bu)-OH, and Fmoc-Val-OH.

General Procedure Coupling Palmitoyl-Cys((*RS*)-2,3-di(palmitoyloxy)-propyl)-OH. Swollen 25 μmol resin loaded with peptide as mentioned was treated with a stock solution of palmitoyl-Cys((*RS*)-2,3-di(palmitoyloxy)-propyl)-OH (0.18 M) and PyBOP (0.22 M) in DCM: NMP (2:1, 1 mL). The resulting mixture was treated with 25 μmol DiPEA at t = 0 and t = 15 min. The resulting suspension was reacted by shaking for 18 h followed by NMP and DCM wash.

General Procedure for Cleavage from the Resin, Deprotection, and Purification. For the cleavage and deprotection the immobilized conjugates were treated with a cleavage cocktail of 95% TFA, 2.5% TIS, and 2.5% H_2O for 60 min. To purify the conjugates, all the precipitates were dissolved in a 1:1:1 mixture of MeCN, ^{t}BuOH, and H_2O and sonicated for 15 min. The mixtures were centrifuged and filtered before injection on the RP-HPLC. The cleavage from the resin, deprotection, and purification by RP-HPLC were performed as previously reported.[8] All isolated conjugates were at least 90% pure as estimated by RP HPLC analysis (See Supporting Information).

*Palmitoyl-Cys((RS)-2,3-di(palmitoyloxy)-propyl)-Ser-Lys-Lys-Lys-Lys-Asp-Glu-Val-Ser-Gly-Leu-Glu-Gln-Leu-Glu-Ser-Ile-Ile-Asn-Phe-Glu-Lys-Leu-Ala-Ala-Ala-Ala-Ala-Lys(i-D-Glu-Ala-MurNAc)-NH_2 (1). **1** (Pam-SLP-MDP).* Twenty-five μmol of crude H-Asp(O^{t}Bu)-Glu(O^{t}Bu)-Val-Ser(O^{t}Bu)-Gly-Leu-Glu(O^{t}Bu)-Gln(Trt)-Leu-Glu(O^{t}Bu)-Ser(^{t}Bu)-Ile-Ile-Asn-(Trt)-Phe-Glu-Lys(Boc)-Leu-Ala-Ala-Ala-Ala-Ala-Lys(Mmt)-Tentagel-S-Ram was elongated with Ser(^{t}Bu)-Lys(Boc)-Lys-(Boc)-Lys(Boc)-Lys(Boc) with standard HCTU/Fmoc chemistry concluding in final Fmoc removal with a solution of 20% piperidine in NMP (4 × 3 min). The resin was treated with Palmitoyl-Cys((RS)-2,3-di(palmitoyloxy)-propyl)-OH in the presence of PyBOP and DiPEA in NMP: DCM (1 mL) for 18 h. The resin was washed (NMP, DCM) and treated with a solution of 3% TFA in DCM. The resin was elongated with standard Fmoc/HCTU chemistry for Fmoc-*i*-D-Gln(OH)-NH_2, Fmoc-Ala-OH. The synthesis was completed with a double coupling of a 2-fold excess of compound **8** preactivated with HATU and DiPEA. To conclude, the resin was treated with a standard cleavage cocktail for 60 min and precipitated with Et_2O. After purification by RP-HPLC title compound **1** was obtained in 2.52 mg (0.55 μmol, 2.2%); LC/MS: Rt = 6.99 min (C_4 Alltima, 50−90% MeCN, 15 min run); ESI-MS: m/z 1533.0 $[M+3H]^{3+}$; 2298.6 $[M+2H]^{2+}$; HRMS Calcd for $[C_{215}H_{374}N_{46}O_{60}S_1 + H]^{4+}$ 1149.69245, found 1149.69466.

*MurNAc-Ala-i-D-Gln-Asp-Glu-Val-Ser-Gly-Leu-Glu-Gln-Leu-Glu-Ser-Ile-Ile-Asn-Phe-Glu-Lys-Leu-Ala-Ala-Ala-Ala-Ala-Lys(Palmitoyl-Cys((RS)-2,3-di(palmitoyloxy)-propyl)-Ser-Lys-Lys-Lys-Lys)-NH_2 (2). **2** (MDP-SLP-Pam).* Twenty-five μmol of crude H-Asp(O^{t}Bu)-Glu(O^{t}Bu)-Val-Ser(^{t}Bu)-Gly-Leu-Glu(O^{t}Bu)-Gln(Trt)-Leu-Glu(O^{t}Bu)-Ser(^{t}Bu)-Ile-Ile-Asn(Trt)-Phe-Glu-Lys(Boc)-Leu-Ala-Ala-Ala-Ala-Ala-Lys-(Mmt)-Tentagel-S-Ram was elongated with standard Fmoc/HCTU chemistry for Fmoc *i*-D-Gln(OH)-NH_2, Fmoc-Ala-OH. The synthesis was completed with a double coupling using a 2-fold excess of compound **8** (preactivated with HATU and DiPEA). The resin was treated with a cleavage cocktail of 3% TFA in DCM and was elongated with Fmoc-Ser(^{t}Bu)-Lys(Boc)-Lys(Boc)-Lys(Boc)-Lys(Boc). The resin was treated with a solution of 20% piperidine in NMP (4 × 3 min). The synthesis was proceeded by treating the resin with a solution of Palmitoyl-Cys((RS)-2,3-di(palmitoyloxy)-propyl)-OH in NMP: DCM (1:1) in the presence of PyBOP and DiPEA for 18 h. The resin was washed (NMP, DCM) and treated with the previously described peptide cleavage and deprotection conditions for 60 min. Purification of the precipitated peptide by RP-HPLC resulted compound **2** (0.94 mg, 0.20 μmol, 0.8%); LC/MS: Rt = 7.06 min (C_4 Alltima, 50−90% MeCN, 15 min run); ESI-MS: m/z 1533.1 $[M+3H]^{3+}$; HRMS Calcd for $[C_{215}H_{374}N_{46}O_{60}S_1 + H]^{3+}$ 1532.58750, found 1532.58780.

Palmitoyl-Cys((RS)-2,3-di(palmitoyloxy)-propyl)-Ser-Lys-Lys-Lys-Lys-Lys(i-D-Gln-Ala-MurNAc)-Asp-Glu-Val-Ser-Gly-Leu-Glu-Gln-Leu-Glu-Ser-Ile-Ile-Asn-Phe-Glu-Lys-Leu-Ala-

DOI: 10.1021/acs.bioconjchem.9b00087
Bioconjugate Chem. 2019, 30, 1150−1161

Ala-Ala-Ala-Ala-Lys-NH_2 (3). ***3*** *(Pam-MDP-SLP).* Twenty-five μmol of crude H-Asp(O^tBu)-Glu(O^tBu)-Val-Ser(^{t}Bu)-Gly-Leu-Glu(O^tBu)-Gln(Trt)-Leu-Glu(O^tBu)-Ser(^{t}Bu)-Ile-Ile-Asn(Trt)-Phe-Glu-Lys(Boc)-Leu-Ala-Ala-Ala-Ala-Ala-Lys-(Boc)-Tentagel-S-Ram was elongated with Ser(^{t}Bu)-Lys(Boc)-Lys(Boc)-Lys(Boc)-Lys(Boc)-Lys(Mmt)-OH according to described HCTU/Fmoc chemistry followed by a coupling of Palmitoyl-Cys((RS)-2,3-di(palmitoyloxy)-propyl)-OH in the presence of PyBOP and DiPEA. The resin was treated with a cleavage cocktail of 3% TFA in DCM and was elongated with standard Fmoc/HCTU chemistry for Fmoc *i*-D-Gln(OH)-NH_2 and Fmoc-Ala-OH. The synthesis was completed with a double coupling using a 2-fold excess of compound **8** preactivated with HATU and DiPEA. The resin was treated with the previously described cleavage and deprotection method for 60 min. Purification by RP-HPLC resulted in compound **3**. (1.2 mg, 0.25 μmol, 1.1%); LC/MS: Rt = 6.27 min (C_4 Alltima, 50−90% MeCN, 15 min run); ESI-MS: *m*/*z* 1575.9 $[M+3H]^{3+}$, 1182.3 $[M+4H]^{4+}$; HRMS Calcd for $[C_{221}H_{386}N_{48}O_{61}S_1 + H]^{3+}$ 1575.28582, found 1575.28635.

MurNAc-Ala-i-D-Gln-Lys(Palmitoyl-Cys((RS)-2,3-di-(palmitoyloxy)-propyl)-Ser-Lys-Lys-Lys-Lys)-Asp-Glu-Val-Ser-Gly-Leu-Glu-Gln-Leu-Glu-Ser-Ile-Ile-Asn-Phe-Glu-Lys-Leu-Ala-Ala-Ala-Ala-Ala-Lys-NH_2 (4). ***4*** *(MDP-Pam-SLP).* Twenty-five μmol of crude N-Asp(O^tBu)-Glu(O^tBu)-Val-Ser(^{t}Bu)-Gly-Leu-Glu(O^tBu)-Gln(Trt)-Leu-Glu(O^tBu)-Ser(^{t}Bu)-Ile-Ile-Asn(Trt)-Phe-Glu-Lys(Boc)-Leu-Ala-Ala-Ala-Ala-Ala-Lys-(Boc)-Tentagel-S-Ram was elongated with standard Fmoc/HCTU chemistry for Fmoc-Lys(Mmt)-OH, Fmoc-*i*-D-Gln-(OH)-NH_2, and Fmoc-Ala-OH. The resin was elongated with a double coupling using a 2-fold excess of compound **8** preactivated with HATU and DiPEA. The resin was treated with a cleavage cocktail of 3% TFA in DCM and the resin was elongated with Fmoc-Ser(^{t}Bu)-Lys(Boc)-Lys(Boc)-Lys(Boc)-Lys(Boc). The resin was treated with a solution of 20% piperidine in NMP. The synthesis was continued by treating the resin with a coupling of Palmitoyl-Cys((RS)-2,3-di-(palmitoyloxy)-propyl)-OH in the presence of PyBOP and DiPEA. After the wash steps (NMP, DCM) the resin was treated with the previously described cleavage and deprotection cocktail for 60 min. Purification by RP-HPLC resulted compound **4**. (1.5 mg, 0.28 μmol, 1.1%); LC/MS: Rt = 6.55 min (C_4 Alltima, 50−90% MeCN, 15 min run); ESI-MS: *m*/*z* 1575.8 $[M+3H]^{3+}$; HRMS Calcd for $[C_{221}H_{386}N_{48}O_{61}S_1 + H]^{3+}$ 1575.62004, found 1575.62140.

H-Asp-Glu-Val-Ser-Gly-Leu-Glu-Gln-Leu-Glu-Ser-Ile-Ile-Asn-Phe-Glu-Lys-Leu-Ala-Ala-Ala-Ala-Ala-Lys(Palmitoyl-Cys-((RS)-2,3-di(palmitoyloxy)-propyl)-Ser-Lys-Lys-Lys-Lys)-NH_2 (2S). ***2S*** *(SLP-Pam).* Tentagel S RAM resin loaded with H-Asp(O^tBu)-Glu(O^tBu)-Val-Ser(^{t}Bu)-Gly-Leu-Glu(O^tBu)-Gln-(Trt)-Leu-Glu(O^tBu)-Ser(^{t}Bu)-Ile-Ile-Asn(Trt)-Phe-Glu-Lys-(Boc)-Leu-Ala-Ala-Ala-Ala-Ala-Lys(Mmt) on 25 μmol was treated 1 M Boc_2O in NMP for 15 min followed by addition of 2 equiv of DiPEA and reacted for another hour. The resin was washed with NMP and DCM. The resin was treated with a cleavage cocktail of 3% TFA in DCM followed by a coupling sequence to elongate the resin with Ser(^{t}Bu)-Lys(Boc)-Lys(Boc)-Lys(Boc)-Lys(Boc). The resin was treated with a solution of 20% piperidine in NMP (4 × 3 min). The resin was treated with Palmitoyl-Cys((RS)-2,3-di(palmitoyloxy)-propyl)-OH in the presence of PyBOP and DiPEA in a NMP:DCM mixture (1:1) for 18 h. The resin was washed (NMP, DCM) and treated with standard cleavage and deprotection conditions. Purification by RP-HPLC yielded compound **2S**. (0.63 mg, 0.16 μmol, 0.62%); LC/MS: Rt = 6.93 min (C_4 Alltima, 50−90% MeCN, 15 min run); ESI-MS: *m*/*z* 1347.1 $[M+3H]^{3+}$, 1010.6 $[M+4H]^{4+}$, 808.6 $[M+4H]^{5+}$ HRMS Calcd for $[C_{193}H_{339}N_{39}O_{50}S + H]^{3+}$ 1346.83932, found 1346.84366.

Cell Culture. Bone marrow derived cells (BMDC) are isolated from WT and $TLR2^{-/-}$ C57BL/6 mice by flushing the bone marrow with complete IMDM culture medium (Lonza), containing 10% FCS (Greiner Bio-one), penicillin/streptomycin (Gibco), L-glutamine (Gibco), and β-mercaptoethanol (Sigma-Aldrich). After culturing for 7 days in complete IMDM culture medium supplemented with 30% supernatant of R1 cultures, as described,[44] BMDCs were fed with fresh medium containing 30% R1 supernatant. BMDCs were used in experiments on day 9 or 10. The D1 cell line is a growth factor-dependent immature splenic DC cell line, derived from C57Bl/6 ($H\text{-}2^b$) mice. D1 cells were cultured as described.[46] The B3Z hybridoma is cultured in complete IMDM medium supplemented with 500 μg/mL hygromycin.[47] The human TLR2- and NOD2-receptor expressing HEK293 cells (Invivogen) were cultured in accordance with the manufacturer's protocol in complete IMDM culture medium supplemented with 10 μg/mL blasticidin. Wild-type HEK293 control cells were cultured in complete IMDM culture medium. Monocyte-derived DCs (moDC) were generated from the $CD14^+$ fraction of PBMC derived from healthy donors. PBMC were isolated over a Ficoll gradient. The $CD14^+$ fraction was isolated from the PBMC using CD14 Microbeads (MACS; Miltenyi). These cells were subsequently cultured in complete RPMI1860 medium (Gibco) in the presence of 800 U/mL GM-CSF and 500 U/mL IL-4 (both Peprotech) for 5 days.

In Vitro DC Activation Assay. Test compounds were titrated in a 96-well plate (Corning) in complete IMDM medium. Next, D1 cells, wild-type BMDC or $TLR2^{-/-}$ BMDC, or moDCs were added to the 96-well plates containing the test compound titrations, using approximately 50 000 cells per well (D1 or moDC) or 20 000 cells per well (BMDC). After 24 h of incubation at 37 °C, supernatant was taken from the wells for ELISA analysis (BioLegend) in which the amount of produced IL-12p40 was measured. After 48 h of incubation at 37 °C, the cells were stained for CD40, CD86, and/or MHC class II (eBioscience) for FACS analysis.

NOD2- and TLR2-Transfected HEK293 Cell Activation. Test compounds were titrated in a 96-wells plate. Approximately 20,000 NOD2-HEK293 or TLR2-HEK293 cells were added per well. After 24 h of incubation at 37 °C, the supernatant was taken from all wells. The amount of IL-8 produced by the NOD2- or TLR2-HEK293 cells, a measure for HEK293 cell activation, was determined using ELISA (Sanquin).

Luminex. Supernatants collected from cell cultures containing any of the described stimulatory compounds were analyzed for the presence of cytokines and chemokines as specified in Figure 3. Luminex technology was applied to measure different analytes in the same sample using a custom multiplex kit (Biorad).

In Vitro T Cell Activation. Naive transgenic OT1 mice were sacrificed at 6−8 weeks of age and spleen and lymph nodes were harvested. After bringing spleen and lymph node cells in suspension, an enrichment for $CD8^+$ T cells was performed by a $CD8^+$ T cell enrichment kit (BD). A high purity (<95%) suspension of OT1 $CD8^+$ T cells was obtained, that are specific for the ovalbumin-derived CTL epitope

DOI: 10.1021/acs.bioconjchem.9b00087
Bioconjugate Chem. 2019, 30, 1150−1161

SIINFEKL. After loading murine D1 DCs with different constructs overnight and subsequent washing of these DCs, the OT1 $CD8^+$ T cells were cocultured for 48 h with the loaded DCs, before addition of 10 μg/mL Brefeldin A for 16 h. The following day, intracellular cytokine staining was performed on the cell cultures and cells were analyzed on a LSRII flow cytometer (BD).

■ ASSOCIATED CONTENT

Supporting Information

The Supporting Information is available free of charge on the ACS Publications website at DOI: 10.1021/acs.bioconjchem.9b00087.

Drawing of the structures of control conjugates and free TLR-ligands, supplementary data on DC-stimulation, data on the activation of nontransfected HEK-cells, LC-MS characterization of the conjugates **1**−**4** (PDF)

■ AUTHOR INFORMATION

Corresponding Authors

*E-mail: filippov@chem.leidenuniv.nl, filippov@lic.leidenuniv.nl (D.V.F.).

*E-mail: f.a.ossendorp@lumc.nl (F.O.).

ORCID

Herman S. Overkleeft: 0000-0001-6976-7005

Jeroen D. C. Codee: 0000-0003-3531-2138

Dmitri V. Filippov: 0000-0002-6978-7425

Notes

The authors declare no competing financial interest.

■ ACKNOWLEDGMENTS

This work has been funded by a Dutch Cancer Society (KWF) grant (UL2007−3906).

■ REFERENCES

(1) Kawai, T., and Akira, S. (2010) The role of pattern-recognition receptors in innate immunity: update on Toll-like receptors. *Nat. Immunol. 11*, 373−384.

(2) Baxevanis, C. N., Voutsas, I. F., and Tsitsilonis, O. E. (2013) Toll-like receptor agonists: current status and future perspective on their utility as adjuvants in improving anticancer vaccination strategies. *Immunotherapy 5*, 497−511.

(3) Lu, H. (2014) TLR Agonists for Cancer Immunotherapy: Tipping the Balance between the Immune Stimulatory and Inhibitory Effects. *Front. Immunol. 5*, 83.

(4) Zom, G. G., Khan, S., Britten, C. M., Sommandas, V., Camps, M. G., Loof, N. M., Budden, C. F., Meeuwenoord, N. J., Filippov, D. V., van der Marel, et al. (2014) Efficient induction of antitumor immunity by synthetic toll-like receptor ligand-peptide conjugates. *Cancer Immunol. Res. 2*, 756−764.

(5) Zom, G. G., Filippov, D. V., van der Marel, G. A., Overkleeft, H. S., Melief, C. J., and Ossendorp, F. (2014) Two in one: improving synthetic long peptide vaccines by combining antigen and adjuvant in one molecule. *Oncoimmunology 3*, e947892.

(6) Maisonneuve, C., Bertholet, S., Philpott, D. J., and De Gregorio, E. (2014) Unleashing the potential of NOD- and Toll-like agonists as vaccine adjuvants. *Proc. Natl. Acad. Sci. U. S. A. 111*, 12294−12299.

(7) Kufer, T. A., and Sansonetti, P. J. (2011) NLR functions beyond pathogen recognition. *Nat. Immunol. 12*, 121−128.

(8) Willems, M. M., Zom, G. G., Meeuwenoord, N., Ossendorp, F. A., Overkleeft, H. S., van der Marel, G. A., Codee, J. D., and Filippov, D. V. (2014) Design, automated synthesis and immunological evaluation of NOD2-ligand-antigen conjugates. *Beilstein J. Org. Chem. 10*, 1445−1453.

(9) Willems, M. M., Zom, G. G., Meeuwenoord, N., Khan, S., Ossendorp, F., Overkleeft, H. S., van der Marel, G. A., Filippov, D. V., and Codee, J. D. (2016) Lipophilic Muramyl Dipeptide-Antigen Conjugates as Immunostimulating Agents. *ChemMedChem 11*, 190−198.

(10) Girardin, S. E., Boneca, I. G., Viala, J., Chamaillard, M., Labigne, A., Thomas, G., Philpott, D. J., and Sansonetti, P. J. (2003) Nod2 is a general sensor of peptidoglycan through muramyl dipeptide (MDP) detection. *J. Biol. Chem. 278*, 8869−8872.

(11) Yoo, Y. C., Saiki, I., Sato, K., and Azuma, I. (1994) MDP-Lys(L18), a lipophilic derivative of muramyl dipeptide, inhibits the metastasis of haematogenous and non-haematogenous tumours in mice. *Vaccine 12*, 175−160.

(12) Boks, M. A., Kager-Groenland, J. R., Haasjes, M. S., Zwaginga, J. J., van Ham, S. M., and ten Brinke, A. (2012) IL-10-generated tolerogenic dendritic cells are optimal for functional regulatory T cell induction–a comparative study of human clinical-applicable DC. *Clin. Immunol. 142*, 332−342.

(13) Fritz, J. H., Le Bourhis, L., Sellge, G., Magalhaes, J. G., Fsihi, H., Kufer, T. A., Collins, C., Viala, J., Ferrero, R. L., Girardin, S. E., et al. (2007) Nod1-mediated innate immune recognition of peptidoglycan contributes to the onset of adaptive immunity. *Immunity 26*, 445−459.

(14) Ribi, E. E., Cantrell, J. L., Von Eschen, K. B., and Schwartzman, S. M. (1979) Enhancement of endotoxic shock by N-acetylmuramyl-L-alanyl-(L-seryl)-D-isoglutamine (muramyl dipeptide). *Cancer Res. 39*, 4756−4759.

(15) Takada, H., and Galanos, C. (1987) Enhancement of endotoxin lethality and generation of anaphylactoid reactions by lipopolysaccharides in muramyl-dipeptide-treated mice. *Infect. Immun. 55*, 409−413.

(16) Fritz, J. H., Girardin, S. E., Fitting, C., Werts, C., Mengin-Lecreulx, D., Caroff, M., Cavaillon, J. M., Philpott, D. J., and Adib-Conquy, M. (2005) Synergistic stimulation of human monocytes and dendritic cells by Toll-like receptor 4 and NOD1- and NOD2-activating agonists. *Eur. J. Immunol. 35*, 2459−2470.

(17) Kawai, T., and Akira, S. (2011) Toll-like receptors and their crosstalk with other innate receptors in infection and immunity. *Immunity 34*, 637−650.

(18) Schwarz, H., Posselt, G., Wurm, P., Ulbing, M., Duschl, A., and Horejs-Hoeck, J. (2013) TLR8 and NOD signaling synergistically induce the production of IL-1beta and IL-23 in monocyte-derived DCs and enhance the expression of the feedback inhibitor SOCS2. *Immunobiology 218*, 533−542.

(19) Tang, L., Zhou, X. D., Wang, Q., Zhang, L., Wang, Y., Li, X. Y., and Huang, D. M. (2011) Expression of TRAF6 and pro-inflammatory cytokines through activation of TLR2, TLR4, NOD1, and NOD2 in human periodontal ligament fibroblasts. *Arch. Oral Biol. 56*, 1064−1072.

(20) Tukhvatulin, A. I., Gitlin, I. I., Shcheblyakov, D. V., Artemicheva, N. M., Burdelya, L. G., Shmarov, M. M., Naroditsky, B. S., Gudkov, A. V., Gintsburg, A. L., and Logunov, D. Y. (2013) Combined stimulation of Toll-like receptor 5 and NOD1 strongly potentiates activity of NF-kappaB, resulting in enhanced innate immune reactions and resistance to Salmonella enterica serovar Typhimurium infection. *Infect. Immun. 81*, 3855−3864.

(21) van Heel, D. A., Ghosh, S., Butler, M., Hunt, K., Foxwell, B. M., Mengin-Lecreulx, D., and Playford, R. J. (2005) Synergistic enhancement of Toll-like receptor responses by NOD1 activation. *Eur. J. Immunol. 35*, 2471−2476.

(22) Hiemstra, I. H., Bouma, G., Geerts, D., Kraal, G., and den Haan, J. M. (2012) Nod2 improves barrier function of intestinal epithelial cells via enhancement of TLR responses. *Mol. Immunol. 52*, 264−272.

(23) Pavot, V., Rochereau, N., Resseguier, J., Gutjahr, A., Genin, C., Tiraby, G., Perouzel, E., Lioux, T., Vernejoul, F., Verrier, B., et al. (2014) Cutting edge: New chimeric NOD2/TLR2 adjuvant drastically increases vaccine immunogenicity. *J. Immunol. 193*, 5781−5785.

DOI: 10.1021/acs.bioconjchem.9b00087
Bioconjugate Chem. 2019, 30, 1150−1161

(24) Takada, H., Yokoyama, S., and Yang, S. (2002) Enhancement of endotoxin activity by muramyldipeptide. *J. Endotoxin Res. 8*, 337−342.
(25) Wiken, M., Grunewald, J., Eklund, A., and Wahlstrom, J. (2009) Higher monocyte expression of TLR2 and TLR4, and enhanced pro-inflammatory synergy of TLR2 with NOD2 stimulation in sarcoidosis. *J. Clin. Immunol. 29*, 78−89.
(26) Ferwerda, G., Girardin, S. E., Kullberg, B. J., Le Bourhis, L., de Jong, D. J., Langenberg, D. M., van Crevel, R., Adema, G. J., Ottenhoff, T. H., Van der Meer, J. W., et al. (2005) NOD2 and toll-like receptors are nonredundant recognition systems of Mycobacterium tuberculosis. *PLoS Pathog. 1*, 279−285.
(27) Kim, Y. G., Park, J. H., Shaw, M. H., Franchi, L., Inohara, N., and Nunez, G. (2008) The cytosolic sensors Nod1 and Nod2 are critical for bacterial recognition and host defense after exposure to Toll-like receptor ligands. *Immunity 28*, 246−257.
(28) Natsuka, M., Uehara, A., Yang, S., Echigo, S., and Takada, H. (2008) A polymer-type water-soluble peptidoglycan exhibited both Toll-like receptor 2- and NOD2-agonistic activities, resulting in synergistic activation of human monocytic cells. *Innate Immun. 14*, 298−308.
(29) Takahashi, Y., Isuzugawa, K., Murase, Y., Imai, M., Yamamoto, S., Iizuka, M., Akira, S., Bahr, G. M., Momotani, E., Hori, M., et al. (2006) Up-regulation of NOD1 and NOD2 through TLR4 and TNF-alpha in LPS-treated murine macrophages. *J. Vet. Med. Sci. 68*, 471−478.
(30) Uehara, A., Yang, S., Fujimoto, Y., Fukase, K., Kusumoto, S., Shibata, K., Sugawara, S., and Takada, H. (2005) Muramyldipeptide and diaminopimelic acid-containing desmuramylpeptides in combination with chemically synthesized Toll-like receptor agonists synergistically induced production of interleukin-8 in a NOD2- and NOD1-dependent manner, respectively, in human monocytic cells in culture. *Cell. Microbiol. 7*, 53−61.
(31) Tada, H., Aiba, S., Shibata, K., Ohteki, T., and Takada, H. (2005) Synergistic effect of Nod1 and Nod2 agonists with toll-like receptor agonists on human dendritic cells to generate interleukin-12 and T helper type 1 cells. *Infect. Immun. 73*, 7967−7976.
(32) Abbott, D. W., Yang, Y., Hutti, J. E., Madhavarapu, S., Kelliher, M. A., and Cantley, L. C. (2007) Coordinated regulation of Toll-like receptor and NOD2 signaling by K63-linked polyubiquitin chains. *Mol. Cell. Biol. 27*, 6012−6025.
(33) Kelsall, B. (2005) Getting to the guts of NOD2. *Nat. Med. 11*, 383−384.
(34) de Oliveira, C. E., Oda, J. M., Guembarovski, L. R., de Oliveira, K. B., Ariza, C. B., Neto, J. S., Hirata, B. K. B., and Watanabe, M. A. (2014) CC chemokine receptor 5: the interface of host immunity and cancer. *Dis. Markers 2014*, 126954.
(35) Deshmane, S. L., Kremlev, S., Amini, S., and Sawaya, B. E. (2009) Monocyte chemoattractant protein-1 (MCP-1): an overview. *J. Interferon Cytokine Res. 29*, 313−326.
(36) Yang, Z., Fuss, I. J., Watanabe, T., Asano, N., Davey, M. P., Rosenbaum, J. T., Strober, W., and Kitani, A. (2007) NOD2 transgenic mice exhibit enhanced MDP-mediated down-regulation of TLR2 responses and resistance to colitis induction. *Gastroenterology 133*, 1510−1521.
(37) Watanabe, T., Asano, N., Murray, P. J., Ozato, K., Tailor, P., Fuss, I. J., Kitani, A., and Strober, W. (2008) Muramyl dipeptide activation of nucleotide-binding oligomerization domain 2 protects mice from experimental colitis. *J. Clin. Invest. 118*, 545−559.
(38) Watanabe, T., Kitani, A., Murray, P. J., and Strober, W. (2004) NOD2 is a negative regulator of Toll-like receptor 2-mediated T helper type 1 responses. *Nat. Immunol. 5*, 800−808.
(39) Watanabe, T., Kitani, A., Murray, P. J., Wakatsuki, Y., Fuss, I. J., and Strober, W. (2006) Nucleotide binding oligomerization domain 2 deficiency leads to dysregulated TLR2 signaling and induction of antigen-specific colitis. *Immunity 25*, 473−485.
(40) Kobayashi, K. S., Chamaillard, M., Ogura, Y., Henegariu, O., Inohara, N., Nunez, G., and Flavell, R. A. (2005) Nod2-dependent regulation of innate and adaptive immunity in the intestinal tract. *Science 307*, 731−734.
(41) Maeda, S., Hsu, L. C., Liu, H., Bankston, L. A., Iimura, M., Kagnoff, M. F., Eckmann, L., and Karin, M. (2005) Nod2 mutation in Crohn's disease potentiates NF-kappaB activity and IL-1beta processing. *Science 307*, 734−738.
(42) Netea, M. G., Ferwerda, G., de Jong, D. J., Jansen, T., Jacobs, L., Kramer, M., Naber, T. H., Drenth, J. P., Girardin, S. E., Kullberg, B. J., et al. (2005) Nucleotide-binding oligomerization domain-2 modulates specific TLR pathways for the induction of cytokine release. *J. Immunol. 174*, 6518−6523.
(43) Borm, M. E., van Bodegraven, A. A., Mulder, C. J., Kraal, G., and Bouma, G. (2008) The effect of NOD2 activation on TLR2-mediated cytokine responses is dependent on activation dose and NOD2 genotype. *Genes Immun. 9*, 274−278.
(44) Khan, S., Bijker, M. S., Weterings, J. J., Tanke, H. J., Adema, G. J., van Hall, T., Drijfhout, J. W., Melief, C. J., Overkleeft, H. S., van der Marel, G. A., et al. (2007) Distinct uptake mechanisms but similar intracellular processing of two different toll-like receptor ligand-peptide conjugates in dendritic cells. *J. Biol. Chem. 282*, 21145−21159.
(45) Chan, W. C., and White, P. D. (1999) *Fmoc solid phase peptide synthesis*, Oxford University Press Inc., New York.
(46) Winzler, C., Rovere, P., Rescigno, M., Granucci, F., Penna, G., Adorini, L., Zimmermann, V. S., Davoust, J., and Ricciardi-Castagnoli, P. (1997) Maturation stages of mouse dendritic cells in growth factor-dependent long-term cultures. *J. Exp. Med. 185*, 317−328.
(47) Sanderson, S., and Shastri, N. (1994) LacZ. inducible, antigen/MHC-specific T cell hybrids. *Int. Immunol. 6*, 369−376.

DOI: 10.1021/acs.bioconjchem.9b00087
Bioconjugate Chem. 2019, 30, 1150−1161